Monovalent, reduced-size quantum dots for imaging receptors on living cells

Mark Howarth[1,3], Wenhao Liu[1], Sujiet Puthenveetil[1], Yi Zheng[1], Lisa F Marshall[1], Michael M Schmidt[2], K Dane Wittrup[2], Moungi G Bawendi[1] & Alice Y Ting[1]

We describe a method to generate monovalent quantum dots (QDs) using agarose gel electrophoresis. We passivated QDs with a carboxy-terminated polyethylene-glycol ligand, yielding particles with half the diameter of commercial QDs, which we conjugated to a single copy of a high-affinity targeting moiety (monovalent streptavidin or antibody to carcinoembryonic antigen) to label cell-surface proteins. The small size improved access of QD-labeled glutamate receptors to neuronal synapses, and monovalency prevented EphA3 tyrosine kinase activation.

To perform single-molecule imaging in cells using dyes or fluorescent proteins, one must constantly contend with a weak signal, which typically bleaches in <10 s. Gold particles or latex beads allow stable single-particle tracking via their scattering, but are generally very large (30–500 nm)[1]. QDs are an alternative probe as they exhibit fluorescence so bright that single molecules can be imaged on an epifluorescence microscope, and their photostability allows hours of illumination without bleaching[2]. However, the full potential of QDs for cellular imaging has not yet been realized because of problems with large QD size (typically 20–30 nm for biocompatible red-emitting QDs[2]), the difficulty of delivering QDs into the cytosol, the instability of antibody-mediated targeting of QDs and QD multivalency. Previously we addressed the problem of binding instability by targeting streptavidin-functionalized QDs to cellular proteins that were site-specifically biotinylated by *E. coli* biotin ligase (BirA)[3]. In this work, we addressed QD multivalency and minimized the size of biomolecule-conjugated QDs (**Fig. 1a**).

QDs that are 20–30 nm can impair trafficking of proteins to which they are attached and restrict access to crowded cellular locations such as synapses[4]. A large fraction of QD size comes from the passivating layer, often a polyacrylic acid polymer or phospholipid micelle[2]. It is challenging to reduce the passivating layer without also increasing nonspecific interactions between QDs and cells, increasing QD self-aggregation and degrading quantum yield[5]. We previously synthesized a coating ligand for CdSe-ZnCdS core-shell QDs (**Supplementary Fig. 1** online) based on a dihydrolipoic acid (DHLA) head group to chelate the ZnCdS shell, 8 ethylene glycol (PEG) units to protect from nonspecific interactions, and a carboxylic acid tail to allow covalent coupling to biomolecules and to confer electrophoretic mobility[6,7]. When we used this DHLA-PEG_8-CO_2H ligand to coat 605 nm–emitting CdSe-ZnCdS QD cores (**Supplementary Methods** online), the resulting small QDs (sQDs) had a hydrodynamic diameter of 11.1 ± 0.1 nm, not much larger than an immunoglobulin gamma antibody (9.7 ± 0.1 nm; **Supplementary Fig. 2a** online). The quantum yield remained high (~40%), and the QDs were stable and monodispersed in PBS (**Supplementary Fig. 2**).

We tested whether the reduction in QD size improved access of the QDs to neuronal synapses. We fused the rat GluR2 subunit of the AMPA-type glutamate receptor, which localizes to postsynaptic membranes, to a 15-amino-acid 'acceptor peptide' (AP) recognition sequence for biotin ligase[3]. Instead of biotinylating the AP on the neuron surface with purified biotin ligase as in previous work[3], we used a simpler protocol in which we transfected neurons with plasmids encoding both AP-GluR2 and an endoplasmic reticulum (ER)-retained BirA construct (BirA-ER; **Supplementary Methods**). Using endogenous ATP and biotin, BirA-ER biotinylates AP-GluR2 in the secretory pathway (**Supplementary Fig. 3** online). We detected biotinylated AP-GluR2 with either streptavidin-conjugated sQDs or commercial streptavidin-QD605 (hydrodynamic diameter 21.2 ± 0.2 nm; **Supplementary Fig. 2a**) and compared the staining to the localization of a post-synaptic marker, Homer-GFP (**Fig. 1b**). AMPA receptors labeled with commercial QDs were hindered from entry into synapses (colocalization 24 ± 6%), whereas AMPA receptors labeled with the sQDs had significantly improved colocalization with the synaptic marker (colocalization 46 ± 7%, $P = 2.1 \times 10^{-4}$). As expected, AMPA receptors labeled using the small-molecule dye Alexa Fluor 568 gave the best colocalization (65 ± 17%).

QD multivalency is also a grave concern, as cross-linking of surface proteins can activate signaling pathways and dramatically reduce receptor mobility[1]. One approach to preparing monovalent nanoparticles had capitalized on the low density of functional sites on polystyrene beads, achieving ~70% monovalency[8,9]. Another approach had used nickel affinity separation, but there was overlap between monovalent and multivalent particles[10]. Nanoparticles have also been separated according to the number of DNA strands attached[11], but this adds a large size and promotes nonspecific binding to cells. Another potential solution is sub-stoichiometric derivatization so that most QDs have no ligand, some have one ligand and very few have two. However, this creates a large

[1]Department of Chemistry, [2]Department of Chemical Engineering and Division of Biological Engineering, 77 Massachusetts Avenue, Massachusetts Institute of Technology (MIT), Cambridge, Massachusetts 02139, USA. [3]Present address: Department of Biochemistry, South Parks Road, Oxford University, Oxford OX1 3QU, UK. Correspondence should be addressed to A.Y.T. (ating@mit.edu).

RECEIVED 7 NOVEMBER 2007; ACCEPTED 24 MARCH 2008; PUBLISHED ONLINE 20 APRIL 2008; DOI:10.1038/NMETH.1206

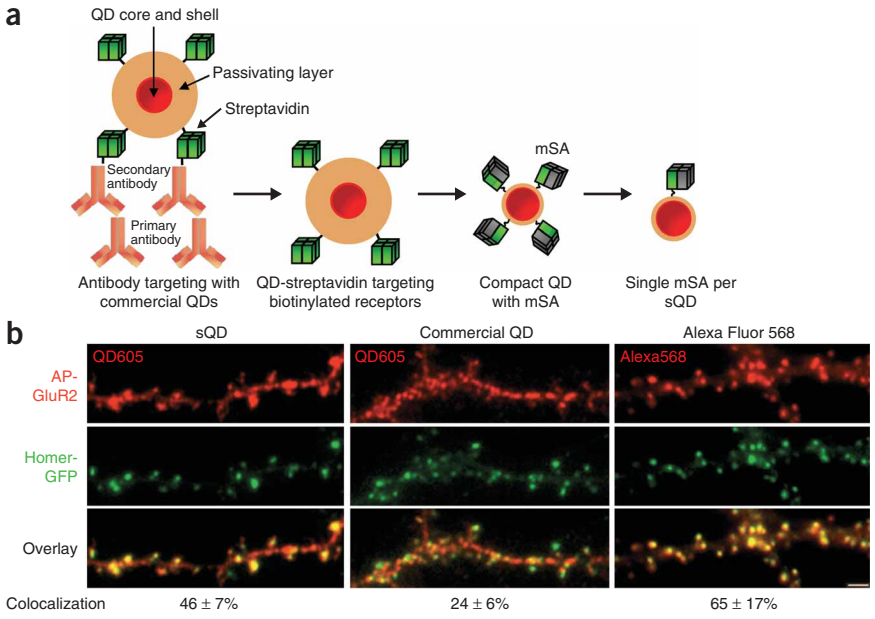

Figure 1 | Overview of small monovalent QDs, and accessibility of sQDs to synapses. (**a**) QDs are typically targeted to cell-surface proteins with antibodies (left), but streptavidin targeting reduces linkage size and increases stability. We decreased QD size by minimizing the passivating layer and reduced cross-linking by conjugating mSA. Finally we purified compact QDs (sQDs) bound to a single copy of mSA. (**b**) Fluorescence images of hippocampal neurons transfected with plasmids encoding AP-GluR2, BirA-ER and the post-synaptic marker Homer-GFP. Biotinylated AP-GluR2 was labeled at the cell surface with sQD-mSA$_1$, commercial QD605-streptavidin, or mSA–Alexa Fluor 568 and imaged live. Yellow shows the overlap between red QD- or Alexa-labeled GluR2, and green Homer puncta. Scale bar, 1 μm. Error, ± 1 s.d. ($n = 6$).

background of untargeted QDs that would be problematic for cytoplasmic labeling, for instance. A complete solution requires QDs uniformly functionalized with exactly one targeting group.

Commercial streptavidin-QD conjugates have 4–10 streptavidin molecules per QD, giving 16–40 biotin binding sites. To generate monovalent sQDs, we first replaced wild-type streptavidin with monovalent streptavidin (mSA), which we had previously engineered to contain a single femtomolar biotin binding site[12] (**Fig. 1a**). The next challenge was to conjugate a single mSA per sQD. Because of their negative charge (zeta-potential = –25 mV), sQDs move rapidly upon electrophoresis in an agarose gel, with comparable mobility to 1 kb DNA. When we conjugated sQDs to mSA and analyzed them by electrophoresis, we observed a striking ladder of QD mobility (**Fig. 2a**). Such a ladder has previously been observed after protein conjugation to QDs, but no purification or characterization had been shown[5,13]. We purified monovalent sQDs (sQD-mSA$_1$, where the subscript indicates the number of copies of mSA per sQD) from the gel by excising the band and centrifuging the sQDs out of the agarose (**Supplementary Methods**). Re-analysis of the purified sQD-mSA$_1$ by electrophoresis showed purity of > 95% (**Fig. 2a**). The hydrodynamic diameter of sQD-mSA$_1$ was 12.3 ± 0.2 nm (**Supplementary Fig. 2a**), only 1.2 nm greater than that of unconjugated sQDs. Although the multivalent metal-affinity interaction between the 6His tag of mSA and the sQD shell is not irreversible, sQD-mSA$_1$ was stable for >4 h at 37 °C as determined by gel electrophoresis and dynamic light scattering analysis (**Supplementary Fig. 4** online).

To test the valency of the gel-purified sQDs, we incubated them with mono-biotinylated DNA at various ratios and analyzed the conjugates by electrophoresis (**Supplementary Methods**). Unconjugated sQDs did not change in mobility, while sQD-mSA$_1$ shifted downward, giving a single new band at both low and high DNA concentrations, consistent with sQD monovalency (**Fig. 2b**). We also assessed valency by atomic force microscopy (AFM) of monovalent or multivalent sQDs (conjugated to ~6 copies of mSA) incubated with a threefold excess of mono-biotinylated DNA (**Fig. 2c** and **Supplementary Methods**). AFM showed monovalent sQD-mSA$_1$ particles bound to a single biotinylated DNA, but multivalent sQDs were bound to multiple DNA strands.

By imaging, we tested the impact of QD monovalency on EphA3, a receptor for ephrin involved in cell movement during development and metastasis. Previous work has shown that binding of EphA3 by multivalent ephrin-coated beads leads to EphA3 clustering and phosphorylation[14]. We labeled CHO cells expressing AP-tagged human EphA3 with either sQD-mSA$_1$ or multivalent sQDs (**Supplementary Methods**). sQD-mSA$_1$ labeled the receptor and remained diffusely localized, but multivalent sQDs clustered AP-EphA3 (**Fig. 3a**). In addition, significantly more EphA3 internalized upon labeling with multivalent sQDs (44 ± 11%)

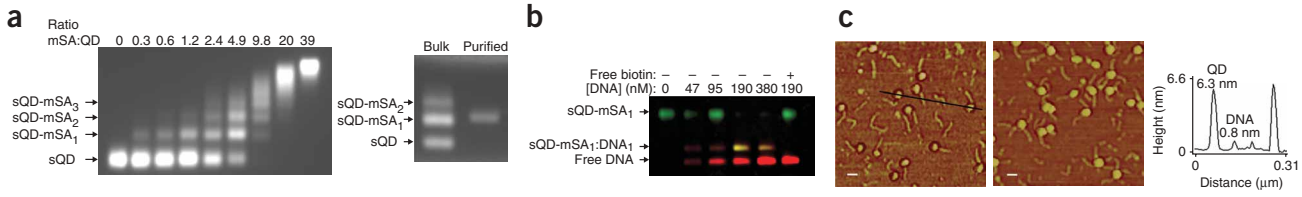

Figure 2 | Generation and characterization of monovalent sQDs. (**a**) sQDs were incubated with mSA, separated on an agarose gel according to the number of mSA molecules attached, and visualized under UV light (left). Discrete bands corresponding to 0–3 copies of mSA per sQD are indicated. sQD-mSA$_1$ was purified from a bulk mixture of sQD-mSA conjugates (right). (**b**) To test valency by gel shift, sQD-mSA$_1$ was incubated with mono-biotinylated DNA and analyzed by agarose gel electrophoresis. In the reaction shown in the rightmost lane, sQD-mSA$_1$ was pre-blocked with free biotin, to test the specificity of QD-DNA binding. QD emission is colored green, DNA is colored red, and yellow shows the overlap. (**c**) To test valency by AFM, purified sQD-mSA$_1$ (left) or multivalent sQDs (right) were incubated with threefold excess mono-biotinylated DNA and imaged by AFM. The height profile along the black line is plotted in the right panel. Scale bar, 25 nm.

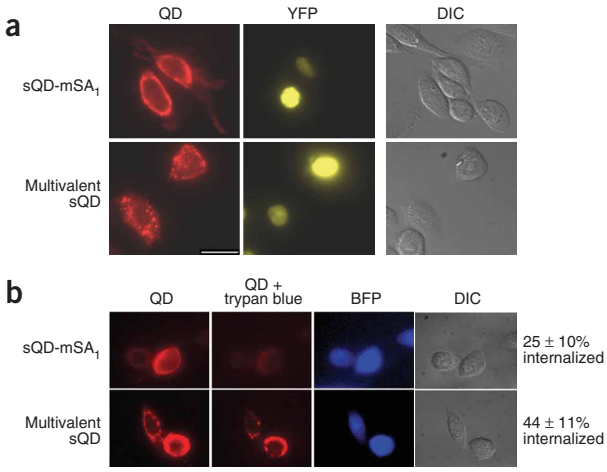

Figure 3 | Monovalent sQDs reduce EphA3 clustering and internalization. (**a**) CHO cells expressing AP-EphA3 were biotinylated and labeled with sQD-mSA$_1$ or multivalent sQDs for 14 min at 37 °C and were imaged live (left). YFP was used as a transfection marker and illustrates that sQD labeling is specific for transfected cells (middle). Differential interference contrast (DIC) images are shown on the right. (**b**) CHO cells expressing AP-EphA3 were biotinylated, incubated with sQD-mSA$_1$ or multivalent sQDs for 14 min at 37 °C, and imaged before and after quenching of surface sQDs with trypan blue. Blue fluorescent protein (BFP) was used as a transfection marker. The percentage internalized sQDs is given as the mean ± 1 s.d. ($n \geq 4$). Scale bars, 10 μm.

compared to sQD-mSA$_1$ (25 ± 10%, $P = 0.021$; **Fig. 3b**), as determined by the quenching of cell-surface sQDs with trypan blue, consistent with receptor activation by multivalent sQDs.

To demonstrate the generality of electrophoretic sQD purification, we also isolated sQDs bound to a single copy of a high-affinity antibody fragment against human carcinoembryonic antigen (CEA; **Supplementary Methods** and **Supplementary Fig. 5** online). We specifically labeled CHO cells expressing CEA with these monovalent anti-CEA sQDs. We found that proteins needed to be >50 kDa to allow electrophoretic separation of sQD conjugates according to valency (data not shown).

We applied sQD-mSA$_1$ to study the mobility of a mutant of low density lipoprotein (LDL) receptor with a truncated cytosolic tail, originally found from an individual with Familial Hypercholesterolemia. This mutant phenotype has been extensively investigated by following LDL, but we analyzed the behavior of the receptor itself (**Supplementary Methods**). We imaged single monovalent sQDs bound to the biotinylated AP-LDL receptor, as indicated by QD fluorescence intensity and blinking. The mobility of mutant receptors labeled with sQD-mSA$_1$ was significantly greater than that of labeled wild-type LDL receptor ($P = 1.6 \times 10^{-14}$; **Supplementary Fig. 6** and **Supplementary Videos 1** and **2** online), consistent with tethering of the wild-type cytosolic tail by adaptors in clathrin-coated pits[15].

Our method of monovalent QD separation has the advantages that it gives high purity, takes less than 30 min, uses commonly available equipment and should be applicable to any protein larger than 50 kDa. Electrophoretic separation also allows easy evaluation of the optimal ligand concentration and the success of the purification. One disadvantage of streptavidin-based protein tracking is that the expression level of the AP fusion protein must be well-controlled. However, our work here demonstrates a method to track endogenous cell-surface proteins without cross-linking, by purifying monovalent antibody-QD conjugates. Our strategy to make monovalent tight-binding QDs, using mSA, could be applied to other nanoparticles that show sufficient electrophoretic mobility. Controlled nanoparticle valency will also be advantageous *in vivo*, where cross-linking can trigger cell lysis, and for bottom-up nanotechnology. The combination of reduced size, monovalency and tight binding could help to make sQD-mSA$_1$ a standard tool for imaging protein dynamics at the single-molecule level.

Note: Supplementary information is available on the Nature Methods website.

ACKNOWLEDGMENTS

Funding was provided by the US National Institutes of Health (NIH) (P20GM072029-01), and the McKnight, the Dreyfus and the Sloan Foundations. M.H. was supported by an MIT-Merck fellowship, W.L. by a US National Science Foundation fellowship, M.G.B. by the Army Research Office DAAD 19-03-D0004, and K.D.W. and M.M.S. by the NIH (CA101830) and the MIT Biotechnology Training Program. We thank M. Lackmann, P. Janes, S. Manalis and A. Sparks for advice, J. Chan for technical assistance, and Tanabe for providing biotin.

AUTHOR CONTRIBUTIONS

M.H., W.L., M.G.B. and A.Y.T. designed the experiments; M.H. and A.Y.T. wrote the paper; M.H., W.L., S.P., L.F.M. and Y.Z. performed the experiments; M.M.S. and K.D.W. generated the PEG-scFv.

COMPETING INTERESTS STATEMENT

The authors declare competing financial interests: details accompany the full-text HTML version of the paper at http://www.nature.com/naturemethods/.

Published online at http://www.nature.com/naturemethods/
Reprints and permissions information is available online at http://npg.nature.com/reprintsandpermissions

1. Saxton, M.J. & Jacobson, K. *Annu. Rev. Biophys. Biomol. Struct.* **26**, 373–399 (1997).
2. Michalet, X. *et al. Science* **307**, 538–544 (2005).
3. Howarth, M., Takao, K., Hayashi, Y. & Ting, A.Y. *Proc. Natl. Acad. Sci. USA* **102**, 7583–7588 (2005).
4. Groc, L. *et al. J. Neurosci.* **27**, 12433–12437 (2007).
5. Pinaud, F., King, D., Moore, H.P. & Weiss, S. *J. Am. Chem. Soc.* **126**, 6115–6123 (2004).
6. Liu, W. *et al. J. Am. Chem. Soc.* **130**, 1274–1284 (2008).
7. Susumu, K. *et al. J. Am. Chem. Soc.* **129**, 13987–13996 (2007).
8. Worden, J.G., Shaffer, A.W. & Huo, Q. *Chem. Commun. (Camb.)* **7**, 518–519 (2004).
9. Sung, K.M., Mosley, D.W., Peelle, B.R., Zhang, S. & Jacobson, J.M. *J. Am. Chem. Soc.* **126**, 5064–5065 (2004).
10. Levy, R. *et al. ChemBioChem* **7**, 592–594 (2006).
11. Fu, A. *et al. J. Am. Chem. Soc.* **126**, 10832–10833 (2004).
12. Howarth, M. *et al. Nat. Methods* **3**, 267–273 (2006).
13. Pons, T., Uyeda, H.T., Medintz, I.L. & Mattoussi, H. *J. Phys. Chem. B.* **110**, 20308–20316 (2006).
14. Wimmer-Kleikamp, S.H., Janes, P.W., Squire, A., Bastiaens, P.I. & Lackmann, M. *J. Cell Biol.* **164**, 661–666 (2004).
15. Michaely, P., Li, W.P., Anderson, R.G., Cohen, J.C. & Hobbs, H.H. *J. Biol. Chem.* **279**, 34023–34031 (2004).

Supplementary Figures

Supplementary Figure 1. Synthesis of QD passivating ligand DHLA-PEG$_8$-CO$_2$H (**5**).

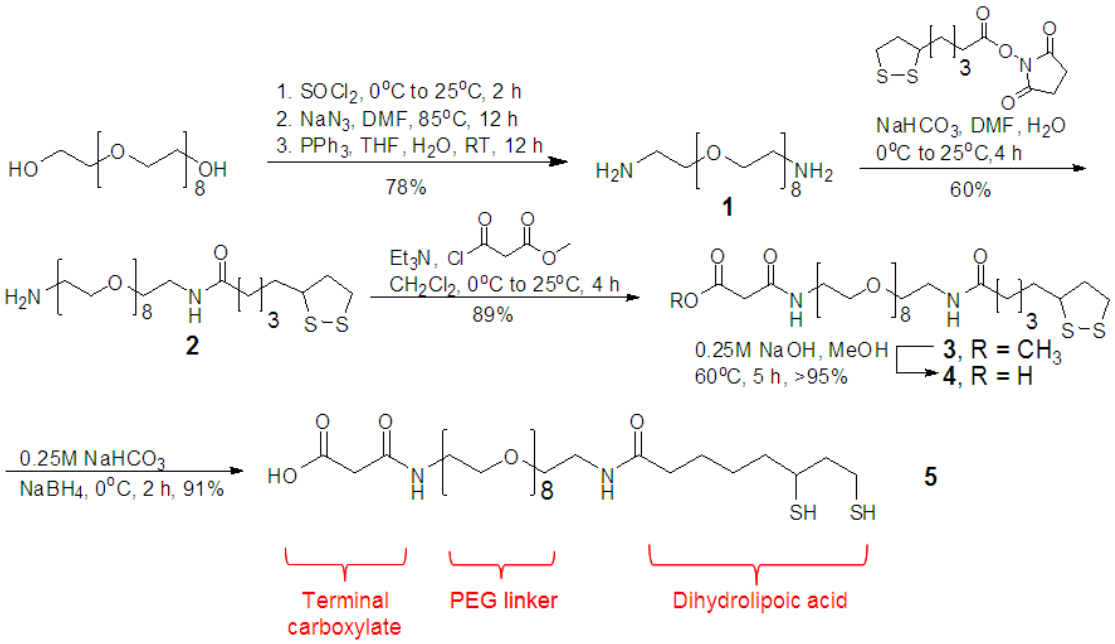

Supplementary Figure 2. Physical characterization of sQDs.

a

Sample	Diameter by DLS (nm)	Diameter by FCS (nm)
sQD	11.1 ± 0.1	10.1 ± 0.6
sQD-mSA$_1$	12.3 ± 0.2	13.4 ± 0.6
Commercial QD-SA	21.2 ± 0.2	23.4 ± 0.8
sQD-mSA$_6$	17.3 ± 0.3	N.D.
IgG antibody	9.7 ± 0.1	N.D.

b

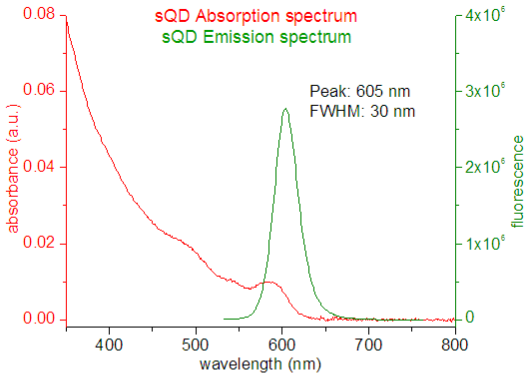

c

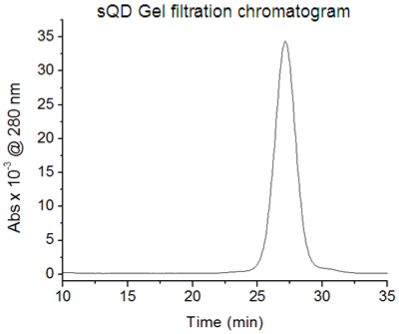

d

mSA:sQD ratio	Relative quantum yield
0	1.00
1	1.12 ± 0.01
6	1.15 ± 0.01

(**a**) Hydrodynamic diameters (mean ± 1 s.d., n = 3) of sQD-mSA$_1$ measured by dynamic light scattering (DLS) and fluorescence correlation spectroscopy (FCS). For comparison, sizes are also shown for the unconjugated small QDs, commercial QDs, multivalent small QDs (sQD-mSA$_6$), and an IgG antibody. (**b**) Absorption (left axis, red) and emission (right axis, green) spectra of sQDs used in this study. FWHM = full width half maximum. (**c**) Gel filtration chromatography to test monodispersity of sQDs in PBS. (**d**) Change in quantum yield after mSA conjugation at a ratio of 1 or 6 mSA per sQD (mean ± 1 s.d., n = 2).

Supplementary Figure 3. Biotinylation of AP fusion proteins by biotin ligase in the endoplasmic reticulum (BirA-ER).

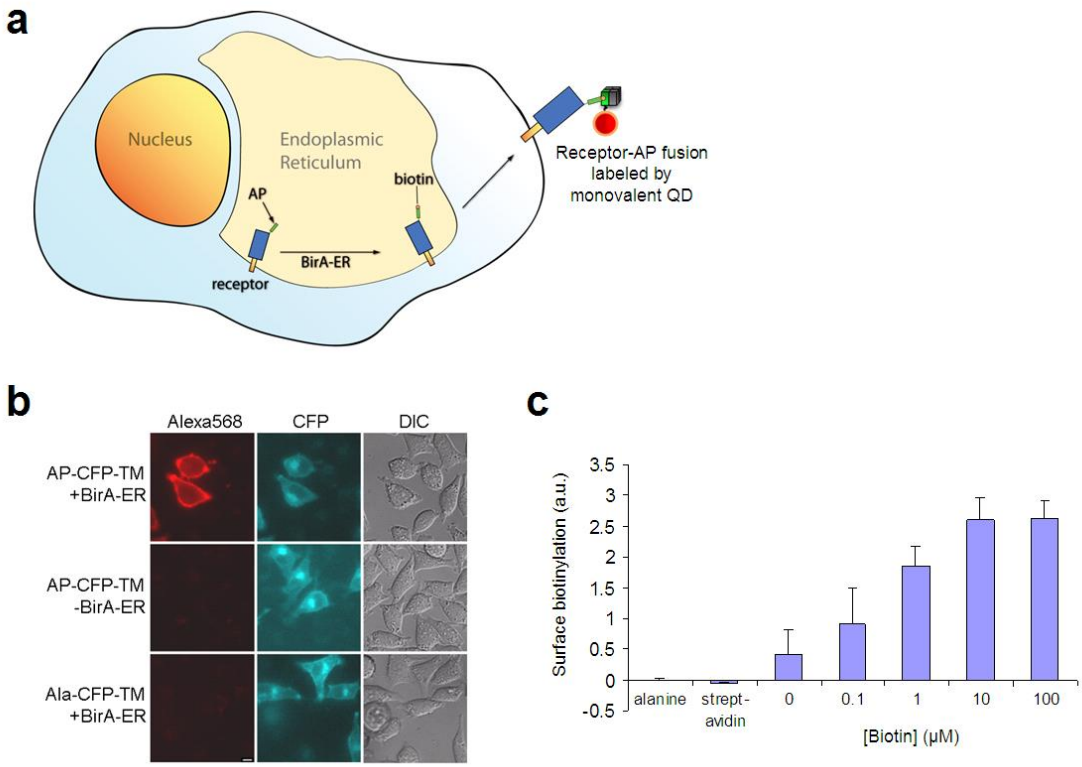

(**a**) Scheme showing site-specific biotinylation with BirA-ER for surface labeling with monovalent QDs. Cells are transfected with the protein of interest genetically fused to a 15-amino acid acceptor peptide (AP). AP is biotinylated by ER-retained biotin ligase. The biotinylated receptor traffics to the cell surface and is bound by the monovalent QD. (**b**) BirA-ER specifically biotinylates AP fusion proteins. HeLa cells were transfected with *AP-CFP-TM* and *BirA-ER*. After incubation overnight in 10 μM biotin, cells were labeled with mSA-Alexa Fluor 568 and imaged live. Negative controls are shown for cells without BirA-ER (middle panel) or with a point mutation in AP stopping biotin ligase recognition (Ala-CFP-TM, bottom panel). Scale-bar 2.5 μm. (**c**) Biotinylation by BirA-ER is modulated by biotin concentration in media. HeLa were transfected with *wild-type AP-GFP-LDL receptor*. After incubation overnight in DMEM + 10% fetal calf serum and varying biotin concentrations, cells were labeled with mSA-Alexa Fluor 568 and imaged live (mean + 1 s.d., n = 3). Biotin depletion from the growth medium used streptavidin-agarose beads ("streptavidin" column). Ala-GFP-LDL receptor ("alanine" column) was a negative control, not recognized by BirA. Biotin in normal growth medium is sufficient for biotinylation of AP fusions in the ER, but 10 μM added biotin gave optimal biotinylation. Biotin even at 1 mM does not cause any apparent change in viability of HeLa or neuronal cultures (data not shown). We confirmed the generality of BirA-ER biotinylation, by using BirA-ER to label the epidermal growth factor receptor and EphA3, each fused to AP, in HeLa cells (data not shown), and to label AP-GluR2 in neurons (**Fig. 1b**).

Supplementary Figure 4. Stability of monovalent sQDs.

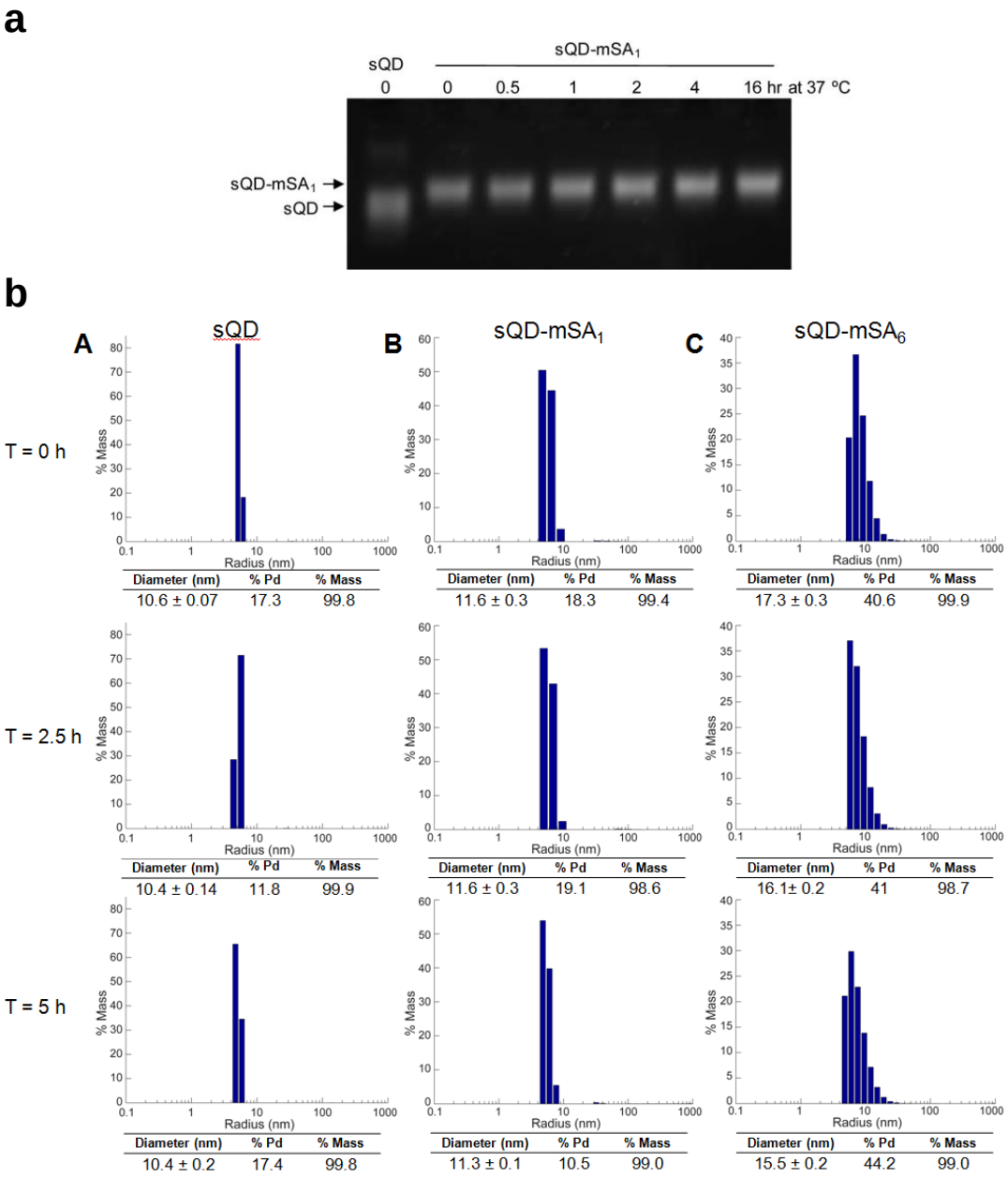

(**a**) Stability of sQD-mSA by electrophoresis. Purified sQD-mSA$_1$ was incubated for varying times at 37 °C and analyzed on a 1% agarose gel, by comparison to unconjugated QDs (sQD) in the same buffer. The monovalent QDs remained stable for at least 4 hr. If there was significant mSA dissociation, one would expect rearrangement of QD-mSA$_1$ to form a mixture including QD-mSA$_0$ and QD-mSA$_2$. (**b**) Stability of sQDs by DLS. sQD (A) and sQD-mSA$_1$ (B) remained monodisperse and stable after 5 hr at 24 °C, with the diameter remaining constant (mean ± 1 s.d., n = 3). sQD-mSA$_6$ (C) also did not aggregate after 5 hr, but the average size gradually decreased. This most likely represents mSA detaching from the QD surface over time, as a result of steric repulsion between multiple mSAs bound to the QD surface. Pd = polydispersity.

Supplementary Figure 5. Generation and testing of monovalent antibody sQDs.

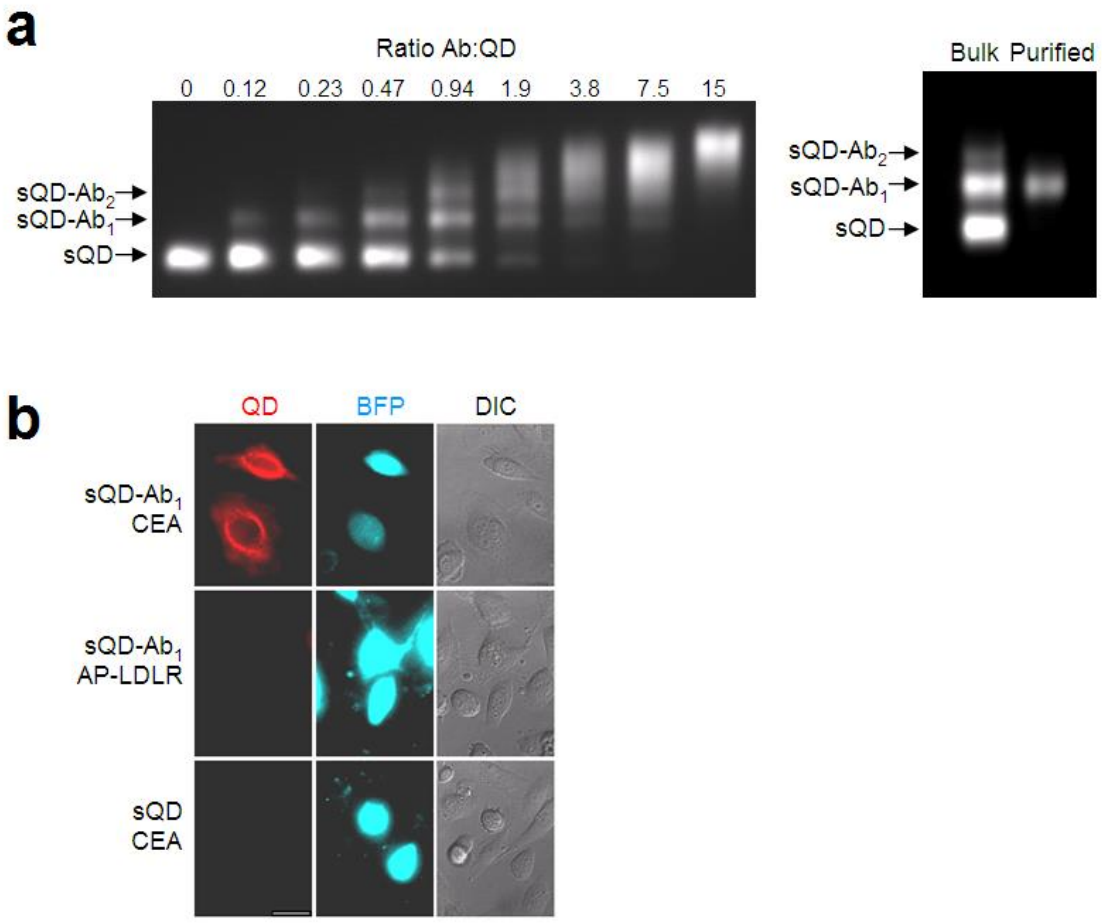

(**a**) Left: Change in sQD mobility according to the number of antibody fragments attached. sQDs were incubated with varying amounts of anti-CEA PEG-scFv antibody (Ab) for 1 h, separated by 1% agarose gel, and visualized under UV. Discrete bands corresponding to 0-2 copies of Ab per sQD are indicated. Right: Monovalent Ab sQDs were purified from a bulk mixture of sQD-Ab conjugates. (**b**) Specific cell labeling with monovalent Ab sQDs. CHO A7 cells were co-transfected with *CEA* and *Blue Fluorescent Protein* (*BFP*). Cells were incubated for 10 min at 4 ºC with 20 nM sQD-Ab_1 and imaged live. As negative controls, cells were transfected with *wild-type AP-LDL receptor* instead of *CEA* (middle row) or were stained with 20 nM unconjugated sQD (bottom row). Scale-bar 10 μm.

Supplementary Figure 6. Single molecule tracking of the LDL receptor with monovalent sQDs.

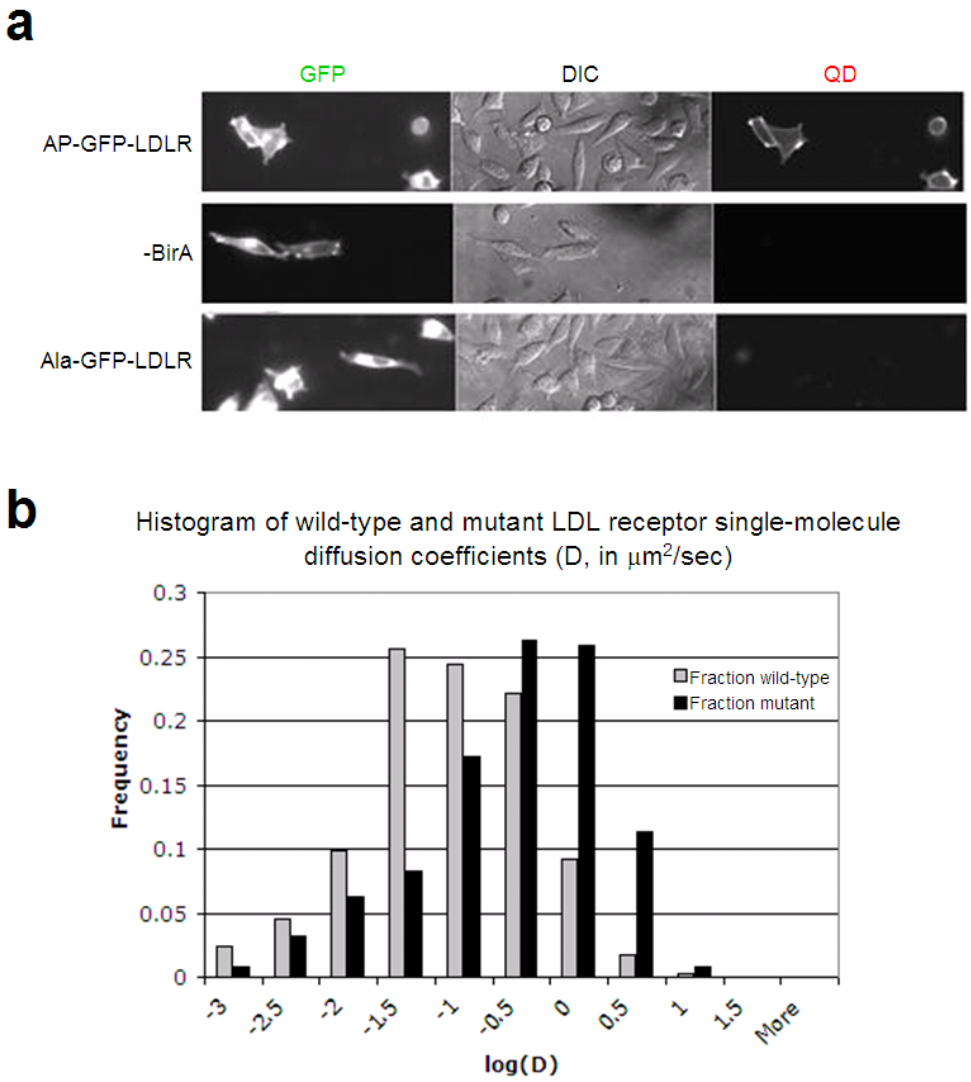

(a) Specificity of cell surface protein labeling with monovalent QDs. HeLa transfected with *AP-GFP-LDLR* were incubated for 5 min with biotin ligase and then stained with sQD-mSA$_1$ for 5 min at 24 ºC. The GFP signal (left column) indicates the transfected cells. DIC (middle column) shows all cells in the field of view. The right column shows QD labeling of AP-GFP-LDLR. In the second row biotin ligase was omitted. In the third row cells were transfected instead with *Ala-GFP-LDLR* (with a point mutation in AP). QD labeling is not seen in the absence of biotin ligase or without AP expression at the cell surface. (**b**) Tracking of wild-type and mutant LDL receptor with monovalent QDs. COS7 cells were transfected with *BirA-ER* and *wild-type* (*WT*) or *mutant AP-LDL receptor*. Biotinylated AP-LDL receptor was labeled with sQD-mSA$_1$ and single QDs were tracked at 37 ºC (Supplementary Videos 1 and 2). Histograms show distinct distributions of single-molecule diffusion coefficients for wild-type and mutant LDL receptor (Kolmogorov-Smirnov D' statistic = 0.32, one sided $P = 1.6 \times 10^{-14}$). Mean log(D) for WT, -1.36 (416 tracks). For mutant, -0.84 (256 tracks).

Supplementary Methods

I. Synthesis of small, monovalent QDs

General

Trioctylphosphine oxide (TOPO), hexadecylamine (HDA), polyethylene glycol (average MW 400 g/mol), *N*,*N*′-dicyclohexylcarbodiimide (DCC), n-hydroxysuccinimide (NHS), dodecanal (DDA), hexamethyldisilathiane ($(TMS)_2S$), (±)-α-lipoic acid, sodium azide, and triphenylphosphine were purchased from Sigma-Aldrich and used as received. n-hexylphosphonic acid (HPA), selenium shot, cadmium 2,4-pentanedionate ($Cd(acac)_2$), and dimethylcadmium ($CdMe_2$) were purchased from Alfa Aesar. Diethylzinc ($ZnEt_2$) was purchased from Fluka. Both $CdMe_2$ and $ZnEt_2$ were filtered through a 0.2 μm filter and stored at -30 °C under inert atmosphere. Trioctylphosphine (TOP) and tributylphosphine (TBP) were from Strem Chemicals. Tributylphosphine selenide (TBP-Se) was prepared by dissolving 0.15 mmol of selenium shot in 100 mL of TBP under inert atmosphere and stirring vigorously overnight, forming a 1.5 M TBP-Se solution. All air-sensitive materials were handled in an Omni-Lab glove box (VAC) under dry nitrogen atmosphere with oxygen levels < 0.2 ppm. All solvents were spectrophotometric grade and purchased from EMD Biosciences. Amine-bearing compounds were visualized on thin layer chromatography (TLC) plates using a ninhydrin solution. All other TLC plates were visualized by iodine staining. NMR spectra were recorded on a DRX 401 NMR Spectrometer (Bruker). Electrospray Ionization Mass Spectrometry (MS) was performed on a QTrap mass spectrometer (Applied Biosystems). Samples for MS were dissolved in a solution of acetonitrile, water, and acetic acid (50:50:0.01 v/v) at a concentration of 2.5 pmol/μL and introduced via syringe pump at a flow rate of 10 μL/min. All polyethylene glycol compounds produced a distribution of molecular weights, separated by 44 m/z. The mass at the maximum of the distribution is reported in the ESI-MS characterization for all samples. UV-Vis absorbance spectra were taken using an HP 8453 diode array spectrophotometer. Photoluminescence spectra were recorded with a SPEX FluoroMax-3 spectrofluorimeter (HORIBA Jobin Yvon). The absorbance of all solutions was maintained below 0.1 optical density (OD) to avoid inner-filter effects.

Synthesis of DHLA-PEG_8-CO_2H ligand (Supplementary Figure 1)

Diamino PEG_8 **1**. Neat PEG_8 (average MW 400 g/mol) (20.0 g, 48.3 mmol) was degassed at 80 ˚C for 1 h with stirring to remove traces of water. The flask was back-filled with N_2 and cooled on an ice bath before thionyl chloride (10.5 mL, 145.0 mmol) was slowly added. The solution was warmed to 25 ˚C and stirred for 2 h. The conversion was monitored by the disappearance of the broad O-H stretch at 3,500 cm^{-1} and the appearance of a C-Cl stretch at 730 cm^{-1} in the IR spectrum. The product was diluted with DMF (20 mL) and the solvent removed under reduced pressure. This was repeated three times to remove all residual traces of thionyl chloride. The sample was dissolved in a solution of sodium azide (9.42 g, 145.0 mmol) in 250 mL DMF and stirred overnight at 85 ˚C. The solvent was removed under reduced pressure and 200 mL of dichloromethane was added. The precipitate was removed by vacuum filtration and the solvent evaporated under reduced pressure to yield the intermediate di-azide. The conversion was confirmed by the appearance of a sharp azide stretch at 2,100 cm^{-1} and the disappearance of the C-

Cl stretch at 730 cm^{-1} in the IR spectrum. The sample was dissolved in 300 mL of tetrahydrofuran (THF), and triphenylphosphine (27.9 g, 106 mmol) was added. The solution was stirred at 25 °C for 4 h before adding 4 mL of water and stirring overnight. The THF was removed *in vacuo* and 100 mL of water was added. The precipitate was removed by vacuum filtration and the filtrate washed with toluene (3 x 50 mL). The water was removed *in vacuo* to yield the pure product as light yellow oil (15.5 g, 78%). ESI-MS: *m/z* 457 $[M + H]^+$. ^1H NMR (400 MHz, $CDCl_3$): δ (ppm) 3.53 (m, 28 H), 3.39 (t, *J* = 5.2 Hz, 4H), 2.74 (t, *J* = 5.2 Hz, 4H), 1.27 (s, 4H).

Lipoic acid NHS ester. To a solution of lipoic acid (5 g, 24.23 mmol) and NHS (3.35 g, 29.1 mmol) in 150 mL THF at 0 ˚C was added slowly a solution of DCC (6.00 g, 29.1 mmol) in 10 mL THF. The mixture was warmed to room temperature and stirred for 5 h. The precipitate was removed by vacuum filtration and the solvent evaporated *in vacuo*. The crude product was re-dissolved in 100 mL of ethyl acetate and filtered once more by vacuum filtration. The product was re-crystallized from a solution of hot ethyl acetate:hexane (1:1 v/v) as a pale yellow solid (5.88 g, 80%). ^1H NMR (400 MHz, CDCl3): δ (ppm) 3.58 (m, 1H), 3.13 (m, 2H), 2.84 (s, 4H), 2.63 (t, *J* = 7.1 Hz, 2H)), 2.50 (m, 1H), 1.99-1.46 (m, 7H).

Lipoic acid-PEG_8-amine **2**. To a solution of **1** (12 g, 29.1 mmol) and sodium bicarbonate (2.44 g, 29.1 mmol) in DMF/water (100 mL, 1:1 v/v) at 0 ˚C was added dropwise a solution of lipoate-NHS ester (1.60 g, 5.27 mmol) in 10 mL DMF over 1 h. The solution was warmed to 25 ˚C, stirred overnight, and extracted with chloroform (3 x 30 mL). The combined organic extracts were washed with water (3 x 30 mL), dried over Na_2SO_4, filtered, and the solvent evaporated. The crude product was purified by alumina column (dichloromethane/methanol 95:5) to give the final product as a yellow oil (1.90 g, 60%). ESI-MS: *m/z* 601 $[M + H]^+$. ^1H NMR (400 MHz, $CDCl_3$): δ (ppm) 3.63 (m, 26H), 3.52 (t, *J* = 5.2 Hz, 2H), 3.47 (t, *J* = 5.2 Hz, 2H) 3.10 (m, 2H), 2.86 (t, *J* = 5.2 Hz, 2H), 2.40 (m, 1H), 2.17 (t, *J* = 6.5 Hz, 2H), 1.99 – 1.46 (m, 7H).

Lipoic acid-PEG_8-CO_2H **4**. To a solution of **2** (1.90 g, 3.16 mmol) and triethylamine (0.640 g, 6.32 mmol) in dichloromethane (30 mL) was dripped slowly a solution of methylmalonylchloride (0.475 g, 3.48 mmol) in dichloromethane (10 mL) at 0˚ C. The solution was stirred at 25 ˚C for 4 h and the solvent removed *in vacuo*. The crude product was purified by silica column (dichloromethane/methanol 95:5) and the solvent evaporated to give the methyl ester **3** as a yellow oil (1.97 g, 89%). Methyl ester deprotection was achieved by stirring with 0.25 M NaOH in MeOH for 5 h at 60 °C. The solvent was removed *in vacuo* after neutralizing to pH 7 with 3.0 M HCl. The product was dissolved in water, acidified to pH 2, and extracted with chloroform (3 x 20 mL) to yield the pure product **4** in quantitative yield. ESI-MS: *m/z* 729 $[M - H]^-$. ^1H NMR (400 MHz, $CDCl_3$): δ (ppm) 3.70-3.52 (m, 36 H), 3.51-3.35 (m, 6H), 3.14 (m, 2H), 2.45 (m, 1H), 2.20 (t, *J* = 7.3 Hz, 2H), 1.96-1.36 (m, 7H).

DHLA-PEG_8-CO_2H **5**. To a solution of **4** (1.50 g, 2.06 mmol) in 0.25 M $NaHCO_3$ (20 mL) at 0 ˚C was slowly added 4 equivalents of sodium borohydride over a 30 min period. The solution was stirred for 2 h on ice, acidified to pH 2 with 3 M HCl, and extracted with chloroform (3 x 15 mL). The combined organic layers were dried over Na_2SO_4 and filtered. The solvent was removed *in vacuo* to yield the product as a colorless oil (1.37 g, 91%). ESI-MS: *m/z* 731 $[M - H]^-$. ^1H NMR (400 MHz, $CDCl_3$): δ (ppm) 3.70-

3.52 (m, 36 H), 3.51-3.35 (m, 6H), 2.87 (m, 1H), 2.65 (m, 2H), 2.18 (t, *J* = 7.3 Hz, 2H), 1.96-1.36 (m, 9H).

Synthesis of CdSe/ZnCdS QD cores

Core-shell CdSe/ZnCdS nanocrystals were synthesized via modification of previously reported procedures[1, 2]. A precursor solution comprising 0.5 mmol $Cd(acac)_2$, 0.25 mL DDA, and 2.8 mL TOP was degassed at 100 ˚C for 1 h, followed by the addition of 3.3 mL of 1.5 M TBP-Se after cooling to 24 ºC. This mixture was loaded into a syringe under dry N_2 atmosphere. In a separate 3-neck round bottom flask, 6.25 g of 90% TOPO and 5.75 g of 90% HDA were degassed at 135 ˚C for 2 h and back-filled with N_2. The temperature was increased to 360 ˚C before rapidly injecting the precursor solution. The temperature was maintained at 280 ˚C until the cores reached a first absorbance maximum at 565 nm. The typical FWHM of the emission spectrum was 28 nm for the cores. After cooling to 80 ˚C, 4 mL of butanol was added to prevent solidification of the product. The sample was allowed to settle for 1 h at 24 ºC and then centrifuged at 3,000 g for 4 min. The pellet was discarded and acetone was added to the colored supernatant to precipitate the cores, followed by another round of centrifugation. The pellet was re-dispersed in hexane, filtered through a 0.2 μm filter, and injected into a degassed solution of 10 g 99% TOPO and 0.4 g n-hexylphosphonic acid. After removing the hexane under reduced pressure at 80 ˚C, the flask was back-filled with dry N_2 and the temperature increased to 130 ˚C before adding 0.25 mL of decylamine and stirring for 30 min. Precursor solutions of $ZnEt_2$/$CdMe_2$ and $(TMS)_2S$ were prepared by dissolving the appropriate amounts of each in 4 mL of TOP and loading them into two separate syringes under inert atmosphere. The amount of $ZnEt_2$ was calculated by assuming a 4 monolayer overcoat according to the methods of Dabbousi[1], with 30% $CdMe_2$ added by mass. Typical masses were 56 mg and 14 mg for $ZnEt_2$ and $CdMe_2$, respectively. A two-fold molar excess of $(TMS)_2S$ was used. The precursor solutions were injected simultaneously into the 130 ˚C bath at a rate of 4 mL/h. Aliquots were removed in 10 min intervals to monitor the red-shift of the photoluminescence spectrum upon over-coating, and the injection was terminated after the desired wavelength was achieved, typically after the addition of three monolayers. The sample was annealed overnight at 80 ˚C, and 4 mL butanol was added. The QDs were stored in growth solution under ambient conditions and centrifuged once more before use. Typical fluorescence quantum yields were 68% for QD605 in hexane.

Preparation of sQDs and analysis of monodispersity (Supplementary Fig. 2c)

Exchange of the native TOPO/TOP surface ligands on QDs for the PEG-derivatized ligand **5** was carried out according to previously reported procedures[3], with several modifications. To 0.2 mL of QDs in growth solution was added MeOH to the point of turbidity. After centrifugation and decantation, 50 μL of neat **5** and 10 μL of MeOH were added. The mixture was stirred at 60 ˚C overnight and precipitated by adding 0.3 mL ethanol, 0.05 mL chloroform, and 0.5 mL hexane in succession. Centrifugation at 3,000 g for 4 min yielded a clear supernatant, from which the ligand was recovered. The pellet was dispersed in 0.5 mL of PBS and filtered through a 0.2 μm filter. The sample was purified using gel filtration chromatography (GFC) in order to narrow the size distribution and concentrated at 3,500 g using a Vivaspin-6 10,000 MWCO spin

concentrator (Vivaproducts). GFC was performed using an ÄKTAprime Plus chromatography system (Amersham Biosciences) equipped with a Superose 6 10/300 GL column. PBS pH 7.4 was used as the mobile phase with a flow rate of 0.5 mL/min. Typical injection volumes were 500 µL. Detection was achieved by measuring the absorption at 280 nm, and the fluorescence spectrum at set time intervals was simultaneously recorded using a SD2000 fiber optic spectrometer with excitation at 460 nm from a LS-450 LED light source (Ocean Optics).

Production of PEG-modified anti-CEA scFv antibody

Secretion vectors for anti-CEA scFv (single-chain variable antibody fragment) sm3E have been described[4]. To prevent protein dimerization, a disulfide bond was inserted between the V_H and V_L domains of the scFv by mutating residues R44 and G234 to cysteine using QuikChange™. QuikChange™ was also used to insert a cysteine at the C-terminus of the scFv, directly preceding the His_6 tag, for PEGylation. Plasmids were transformed into YVH10 yeast using the EZ Yeast Kit (Zymo Research) and plated on SD-CAA media supplemented with 40 µg/mL tryptophan. Individual colonies were grown in 1 L flasks and secretion induced for 48 h at 37 ºC as described[4]. The cleared supernatant was concentrated using a 10 kDa ultrafiltration membrane (Millipore) and the His-tagged protein purified with Talon metal affinity resin (BD Biosciences) following the manufacturer's batch-column protocol. Monomeric scFv was further purified by size exclusion chromatography on a Superdex 75 column (GE Healthcare) and eluted into PEGylation buffer (100 mM Na_2HPO_4, 500 mM NaCl, 2 mM EDTA, pH 6.5). Unmodified scFv was too small (28.1 kDa) to give discrete bands after conjugation to QDs (data not shown), but PEGylation of the scFv significantly increased the effective hydrodynamic size, without impairing antigen recognition. For PEGylation, scFv at a concentration of 0.5–1 mg/mL was co-incubated with a 5 fold molar excess of 5 kDa PEG-maleimide (Nektar) and immobilized tris[2-carboxyethyl]phosphine hydrochloride (TCEP) reducing gel (Pierce) at a concentration of 150 µL gel per 1 mL reaction. Using TCEP resin instead of soluble TCEP or dithiothreitol to reduce the C-terminal cysteine prevented reduction of the partially buried disulfide bonds in the protein. The reaction mixture was incubated at 25 ºC for 5 h on a rocker. The TCEP resin was then removed by centrifugation. Unreacted PEG was removed by ion exchange chromatography on a Hi-Q column (GE Healthcare) equilibrated with 20 mM Tris HCl, pH 8.2. PEGylated scFv was separated from unconjugated scFv on a Superdex 75 column at a flow rate of 0.5 mL/min and eluted in PBS. The purified PEG-scFv conjugate had an effective molecular weight of ~60 kDa as measured by size exclusion chromatography, as a result of the large hydrodynamic radius of the linear PEG. The PEGylation efficiency and conjugate purity were assessed by SDS-PAGE. scFv protein concentration was determined from A_{280}, using the ε of 50,225 $M^{-1}cm^{-1}$ calculated from ExPASy Protparam.

Purification and electrophoretic analysis of monovalent sQDs (Figure 2a, Supplementary Figure 4a and Supplementary Figure 5a)

8 µM sQDs in PBS were incubated with the indicated volumes of monovalent streptavidin (mSA, 19 µM) or PEG-scFv antibody (13 µM) in PBS in a total volume of 5 µL for 1 h at 24 ºC. mSA was prepared as described[5, 6]. mSA and PEG-scFv each contained a single His_6-tag that stably binds to the ZnCdS shell[7]. Addition of 1-ethyl-3-

diisopropylaminocarbodiimide did not change the conjugation efficiency (data not shown). Analysis of QD-protein conjugation was performed by electrophoresis using a Minicell Primo (Thermo) with 1% Omnipur agarose (EMD) in 10 mM $Na_2B_4O_7 \cdot 10H_2O$ (adjusted to pH 8.0 using 1 M HCl) at 7.9 V/cm for 15 min. 6x loading buffer (16% sucrose in ddH_2O) was added to samples before loading. For purification, buffer was cooled on ice, the electrophoresis apparatus was surrounded in ice, and the gel was run at 6.4 V/cm for 20 min. Gels were visualized under 305 nm UV with a ChemiImager 5500 (Alpha Innotech Corporation) for analysis, or with the naked eye under ambient light for purification. Bands of interest were excised with a scalpel, placed in a Nanosep MF 0.2 μm filter (Pall), and centrifuged at 5,000 g for 1 min at 24 ºC. This centrifugation eluted the buffer and QD-protein conjugates from the agarose into the collecting tube below. Band purity was quantified with ChemiImager 5500 software. Typically, sQD-mSA_1 preps started from 120 pmol sQDs and 120 pmol mSA. Conjugation with mSA is stochastic and so ~40 pmol were monovalent. Extraction efficiency from agarose was 30-50% (data not shown), giving a typical final yield of ~12-20 pmol sQD-mSA_1.

For Supplementary Figure 4a, sQD and sQD-mSA_1 at 40 nM were incubated in 10 mM sodium borate pH 7.3 with 0.1% BSA for varying times at 37 °C and analyzed by electrophoresis on a 1% agarose gel.

II. Characterization of QDs

Dynamic Light Scattering measurements of QD size (Supplementary Figure 2a and Supplementary Figure 4b)

QD size was measured using a DynaPro™ Dynamic Light Scatterer (DLS) (Wyatt Technology Corporation). All samples were at 0.5-2 μM and filtered through a Nanosep MF 0.2 μm filter (Pall) before analysis. Typical count rates were 85-150 kHz. Each autocorrelation function was acquired for 10 s, and averaged for 10 min per measurement. A software filter was employed to discard all autocorrelation function fits with sum of squares errors >15. The resulting autocorrelation function was fitted using Dynamics V6 software (Wyatt Technology Corporation), employing a non-negative least squares fitting algorithm. Hydrodynamic diameter was obtained from a mass-weighted size distribution analysis and reported as the mean of triplicate measurements. The antibody used for DLS was a mouse IgG1 to the truncated Nerve Growth Factor Receptor, obtained by Protein G affinity purification from the supernatant of B cell hybridoma 8737 (ATCC) and dialyzed into PBS.

Fluorescence correlation spectroscopy (FCS) measurements of QD size (Supplementary Figure 2a)

Two-photon FCS measures the autocorrelation of the emission of QDs in solution under a microscope objective, to determine the dynamics of time spent in a calibrated focal volume and therefore the diffusion constant[8]. Diffusion constant is then related to hydrodynamic diameter via the Stokes-Einstein relation. The home-built instrument begins with 780 nm light from a coherent Ti-Sapphire oscillator pumped with an Ar+ ion laser (Coherent Mira) and operating with a pulse-width of ~120 fs and a repetition rate of 80 MHz. The beam is sent through a 40x, 1.2 NA water immersion objective (Zeiss). Fluorescence is collected through the same objective, filtered through a 720 nm longpass

dichroic (Chroma), 400 nm holographic notch filter and an appropriate bandpass. Then, the light passes through a 50/50 beam splitter to two avalanche photodiodes (EG&G and SPCM-AQR14). The signal is cross-correlated by a multi-tau autocorrelator card (ALV GmbH). This cross-correlation reduces the noise of the measurement and eliminates artifacts from the after-pulsing of the photodiodes. The 3D focal volume waist and aspect ratio is calibrated according to a standard 3D Gaussian approximation. The aspect ratio is first calculated using a known concentration of R_H = 22 nm beads (Duke Scientific, product G40). This ratio is then applied to a series of freshly filtered beads (R_H = 22 nm, 28.5 nm, 35.5 nm, 44 nm, Duke Scientific, G40, G50, G75, G80) to determine the beam waist. r^2 values for these fits were > 0.999. Samples were measured with a range of excitation powers, to ensure that we were not in a regime where blinking, saturation, and photobleaching would influence the measurements[9]. For the final measurement, sQDs were excited with 0.75 mW on the back focal plane of a lightly over-filled objective and the commercial QD605-SA sample was excited with 0.5 mW. Samples were measured for 10 runs of 30 s each and the r^2 values were > 0.998 for the average curve. Hydrodynamic diameter was calculated as described[10].

Measurement of quantum yield (Supplementary Figure 2d)

Quantum yield (QY) was measured relative to Rhodamine 640 with excitation at 520 nm. Solutions of QDs in PBS and dye in ethanol were optically matched at the excitation wavelength. Fluorescence spectra of QD and dye were taken under identical spectrometer conditions in triplicate and averaged. The optical density at the peak was kept below 0.1 [11], and the integrated intensities of the emission spectra, corrected for differences in index of refraction and concentration, were used to calculate QY using the expression

$$QY = \left(\frac{Abs_{dye}}{Abs_{QD}}\right)\cdot\left(\frac{n_{QD}^2}{n_{dye}^2}\right)\cdot\left(\frac{S_{QD}}{S_{dye}}\right)\cdot QY_{dye}$$

where *Abs* is the absorbance at 490 nm, *n* is the refractive index of the solvent (water for QD, and ethanol for dye), *S* is the integrated area under the fluorescence spectrum, and QY_{dye} is the absolute QY reported for rhodamine 590 (99% in ethanol).

For relative QY measurements, sQDs (8 µM) were incubated with various ratios of mSA in PBS for 30 min at 24 ºC. Aliquots were diluted 25x in PBS and loaded onto a 96-well plate for fluorescence analysis. The fluorescence intensity was measured using a XFluor4 plate reader (Tecan) with excitation at 450 nm and emission at 605 nm. Error bars represent ± 1 s.d. from duplicate measurements. 100% increases in QD photoluminescence have previously been observed after conjugation of His-tagged proteins, which is attributed to the His-tag coordinating with surface sites on the QD shell and improving the QD passivation[12].

Zeta-potential measurement

Zeta-potential was measured on a Zeta PALS Zeta Potential Analyzer (Brookhaven Instruments Corporation). sQDs were measured at 3µM in PBS. Values are reported as the average of triplicate runs consisting of 100 scans each.

Gel shift analysis of QDs with mono-biotinylated DNA (Figure 2b)

236 bp mono-biotinylated DNA was generated by PCR from pIVEX-BirA (a gift from A. Griffiths, MRC Laboratory for Molecular Biology) using Taq DNA polymerase with the primers 5' biotin-triethylene glycol-GCGTTGATGCAATTTCT (Eurogentec) and primer S (5'TGGCTGCTGCCACCGCTG), using the conditions 95 ºC 30 s, 50 ºC 30 s, 72 ºC 1 min for 27 cycles. The PCR product was purified from a 2% agarose gel using a QIAquick gel extraction kit (Qiagen). Varying amounts of 190 nM mono-biotinylated DNA were incubated in 100 mM sodium borate pH 8.0 for 10 min at 24 ºC with 60 nM sQD-mSA$_1$. To visualize QDs and DNA separately, we used sQDs emitting at 545 nm, generated exactly as for sQDs emitting at 605 nm but with smaller CdSe cores[13]. As a negative control to block DNA binding, sQD-mSA$_1$ was pre-incubated for 5 min with 10 μM biotin. Samples were then mixed with 6x loading buffer (16% sucrose in ddH_2O) and run using a Minicell Primo (Thermo) on a 0.9 % Omnipur agarose (EMD) gel, cast with 0.5 μg/mL ethidium bromide, at 7.9 V/cm for 15 min in TAE buffer. Gels were visualized under 365 nm UV with a ChemiImager 5500, using an ethidium bromide filter (Alpha Innotech) to see DNA, and a GFP filter (Alpha Innotech) to see sQDs.

AFM of QDs (Figure 2c)
119 bp mono-biotinylated DNA was prepared by PCR as above, except primer S was replaced with primer XS (5'GTCGCCATGATCGCGTAGT). 9 nM of this mono-biotinylated DNA, prepared as above, was incubated with 3 nM QD sample for 1 h at 24 ºC in 10 mM sodium borate pH 7.3. 20 μL 0.1 % poly-L-lysine (MW 500-2000) (Sigma) was pipetted on freshly cleaved muskovite mica V2 (Electron Microscopy Sciences). After incubation for 3 min, the mica was washed with 1 mL of water and dried in a nitrogen stream. 20 μL DNA-QD complex was pipetted onto the mica. After 6 min, the mica was rinsed with 1 mL of water and dried in a nitrogen stream. The mica was imaged using a Dimension 3100 AFM (Digital Instruments) in tapping mode, using an etched TESP silicon probe with a nominal tip radius of < 10 nm (Veeco Probes) operating at a resonant frequency of 273.3 kHz. Height and phase images were collected simultaneously across a 1 x 1 μm area, at a scan rate of 2 Hz and a resolution of 256 x 256 pixels. The resulting images were analyzed using Nanoscope v 5.30 software (Digital Instruments) and the phase image is displayed.

III. Plasmids

General plasmids
AP-GluR2 in CMVbipep-neo, encoding the *rat GluR2 AMPA receptor subunit* fused to *AP*, has been described[14]. The post-synaptic marker *Homer-GFP* (*rat Homer1b* fused to *GFP* in pCI) was a gift from Y. Hayashi (MIT). *AP-EphA3* in pEF-BOS was a gift from M. Lackmann (Monash University). *AP* was inserted by Quikchange™ (Stratagene) immediately after the signal sequence of *human EphA3*, using the primer 5'GTTCTCGACAGCTTCGGGGGCCTGAACGATATCTTCGAGGCCCAGAAGATCGAGTGGC ACGAGGAACTGATTCCGCAGCC and its reverse complement. The nuclear co-transfection marker *pEYFP-H2B* (*human histone H2B* fused to *EYFP*)[15] was a gift from A. K. Leung (MIT). The cytoplasmic co-transfection marker *BFP* was a gift from R. Y. Tsien (UCSD). *Human carcinoembryonic antigen* (CEA) in pIRES was a gift from G.

Prud'homme (University of Toronto). *AP-CFP-TM* and *Ala-CFP-TM* in pDisplay have been described[16].

Cloning of BirA-ER
BirA-YFP-ER has the following structure: Ig signal sequence-HA tag-BirA-YFP-KDEL. *BirA* was amplified using the primers 5'GCATAGATCTATGAAGGATAACACCGTG and 5'ACCTGGCTTCCCAGATCCAGATGTAGACCCTTTTTCTGCACTACGCAG. *YFP* was amplified with the primers 5'GGATCTGGGAAGCCAGGTTCTGGTGAGGGTATGGTGAGCAAGGGCGAG and 5'ATGGGTCGACCTTGTACAGCTCGTCCAT. *BirA* was joined to *YFP* using extension overlap PCR. The product was gel-purified and ligated into the *BglII* and *SalI* sites of pDisplay (Invitrogen), to give *BirA-YFP-TM*. To generate *BirA-YFP-ER*, Quikchange™ using the primer 5'GCATGGACGAGCTGTACAAGGGTTCAAAGGACGAGCTGTGAGTCGACGAACAAAAACT CATC and its reverse complement was performed on *BirA-YFP-TM*, inserting KDEL (a tetrapeptide promoting ER retention[17]) and a stop codon after *YFP*. To generate *BirA-ER*, *YFP* was deleted from *BirA-YFP-ER* by Quikchange™ using the primer 5'GGGTCTACATCTGGATCTGGGGGTTCAAAGGACGAGCTGTGAGTCG and its reverse complement. Related constructs targeting BirA to the secretory pathway have been previously described[18-20].

Cloning of AP-LDL receptor
Human LDL receptor in pEGFP was a gift from T. Kirchhausen (Harvard). *AP* was inserted by inverse PCR[21] with the primers 5'CTTCGAGGCCCAGAAGATCGAGTGGCACGAGACTGTGAGCAAGGGCGAGGAG and 5'ATATCGTTCAGGCCACTTCTGTCGCCAACTGCAG, to give *AP-GFP-LDL receptor*. *Ala-GFP-LDL receptor* contains a lysine to alanine point mutation in AP, to block biotinylation, and *AP* was mutated as previously described[16].
GFP was removed from *AP-GFP-LDL receptor* by QuikChange™ with the primer 5'CCCAGAAGATCGAGTGGCACGAGGGGGGAGAATTCGACAGATGTG and its reverse complement, to give *wild-type AP-LDL receptor*, so that *AP* is located directly after the signal sequence. *Mutant AP-LDL receptor* containing the Familial Hypercholesterolemia mutation Trp792Stop[22, 23], also known as FH683, was generated by Quikchange™ using the primer 5'CCTTCTATGGAAGAACTGACGGCTTAAGAACATCAAC and its reverse complement.

IV. Cell labeling and imaging

General cell culture
CHO ldlA7 (A7) are a variant of CHO lacking endogenous LDL receptor[24] and were a kind gift from M. Krieger (MIT). COS7, CHO, HeLa and A7 were grown in DMEM with 10% Fetal Calf Serum, 50 U/mL penicillin, 50 μg/mL streptomycin, 1 mM pyruvate and L-proline at 69 mg/L (growth medium). DMEM is reported to contain no biotin (Invitrogen) and 100% Fetal Calf Serum contains ~ 90 nM biotin[25]. To deplete biotin, the growth medium was incubated with streptavidin-agarose slurry (Novagen) (100 μL per 1

mL medium) for 30 min at 24 ºC with rocking, before pelleting the slurry and sterile-filtering the supernatant. Cell-lines were transfected using 1 μL Lipofectamine 2000 (Invitrogen), 0.1 μg of the gene of interest and 5 ng co-transfection marker per well of a 48-well plate. Where cells were cotransfected with *BirA-ER* and an *AP fusion*, 0.1 μg of each plasmid was used per well. Cells were imaged the day after transfection. Primary hippocampal cultures were prepared from E18-19 rats, in accordance with MIT guidelines. Briefly, hippocampi were dissociated with papain and neurons were plated onto 12 mm coverslips in Basal Medium Eagle (BME) plus 5% Fetal Calf Serum at a density of 200,000 cells/well. The coverslips were pre-coated with 0.1 mg/mL poly-D-lysine (MW 300,000) (Sigma) and 5 μg/mL mouse laminin (Invitrogen) overnight. After cultures were grown at 37 °C for 8 h, the medium was replaced with Neurobasal medium (Invitrogen) supplemented with 2% B27 (Invitrogen), 0.5 mM glutamine, 25 U/mL penicillin and 25 μg/mL streptomycin for further culture. Neurons were transfected using calcium phosphate at DIV6.

Receptor biotinylation (Figure 3, Supplementary Figure 3 and Supplementary Figure 5b)
For biotinylation by recombinant biotin ligase, cells were incubated in PBS 5mM $MgCl_2$ with 2.6 μM biotin ligase and 10 μM biotin-AMP at 24 ºC for 10 min, as previously described[5, 6]. Cells were then washed 4x with PBS and incubated for 5 min at 24 ºC with 20 nM QDs in PBS with 0.5% dialyzed bovine N,N-dimethyl casein (Calbiochem). Cells were washed 3x in PBS and imaged in PBS at 24 ºC. For imaging of cells expressing BirA-ER[19, 20], cells were incubated in growth medium supplemented with 10 μM biotin (Tanabe USA) from 4 h after transfection. The next day cells were washed 4x in PBS and incubated for 5 min at 24 ºC with 20 nM monovalent QDs in PBS with 0.5% casein. For specificity testing, cells were incubated with monovalent streptavidin-Alexa Fluor 568, prepared as described[5] at 100 nM in PBS with 1% dialyzed Bovine Serum Albumin for 10 min at 4 ºC. Cells were then washed 3x in PBS and imaged live.

For analysis of AP-EphA3 clustering and internalization, cells were biotinylated by recombinant biotin ligase as above for 10 min, washed 3x in PBS and then incubated with 10 nM monovalent or multivalent QD in PBS with 0.5% casein for 14 min at 37 ºC. Cells were washed 3x in ice-cold PBS and imaged at 4 ºC. Trypan blue (Invitrogen), a membrane-impermeable dye, was then added to the imaging medium to a final concentration of 42 μM, which immediately quenched fluorescence of cell surface QDs, and the cells were re-imaged with the same microscope settings. Trypan has been widely used to quench cell surface fluorescence of small molecule fluorophores[26, 27]. In Slidebook (Intelligent Imaging Innovations), regions were gated based on where the BFP fluorescence was above background and QD fluorescence was determined for these regions, after subtracting the QD signal from a region where there were no cells. Internalization was calculated as: (QD fluorescence after trypan blue)/(QD fluorescence before trypan blue) x 100. Mean internalization was calculated from 4-6 cells taken from different fields and is given ± 1 s.d. .

General imaging
Cells were imaged using an Axiovert 200M inverted epifluorescence microscope (Zeiss) with a 40x oil-immersion lens, a Cascade II camera (Photometrics) with intensification set at 4095, and a halogen lamp. BFP (420DF20 excitation, 450DRLP dichroic, 475DF40

emission), YFP and GFP (495DF10 excitation, 515DRLP dichroic, 530DF30 emission), Alexa Fluor 568 (560DF20 excitation, 585DRLP dichroic, 605DF30 emission), and QD605 (405DF20 excitation, 585DRLP dichroic, 605DF30 emission) images were collected and analyzed using Slidebook software. Typical exposure times were 0.1-0.5 s. Fluorescence images were background-corrected. Different samples in the same experiment were prepared, imaged and analyzed under identical conditions. For acquiring videos, cells were maintained at 37 ºC using an environmental control system (Solent Scientific). Videos were acquired with 0.2 s exposure and no delay between frames, using an additional 2.5x Optovar lens. QDs were tracked using Slidebook with automatic particle identification and a maximum movement per timepoint of 2 μm. Diffusion coefficients (D) were calculated in Slidebook by a linear fit to the first 4 points of the plot of Mean Squared Displacement versus time. To determine if the two distributions of LDL receptor mobility differed, significance was determined from tracks with $D > 0$ and path-length between 2 and 25, using a one-sided Kolmogorov-Smirnov test statistic (D'), which was implemented in R (http://www.r-project.org/).

Biotinylation by BirA-ER was calculated by dividing the median Alexa Fluor 568 intensity by the median GFP intensity for each transfected cell, to normalize for expression level, and is shown as the mean biotinylation level (in arbitrary units, a.u.) from 3 fields of view + 1 s.d.

Synaptic localization of QD-labeled AMPA receptors (Figure 1b)

Neurons were transfected using calcium phosphate at DIV6 with 0.4 μg *Homer-GFP*, 0.8 μg *BirA-ER* and 1.6 μg *AP-GluR2* per well of a 24-well plate. On DIV19 the neurons were washed 3x in Tyrode's buffer and incubated in Tyrode's with 0.5 % casein and 0.2 nM commercial QD605-SA[28] (Invitrogen cat # Q10101MP, PEG-amine streptavidin-QD605) or 20 nM sQD, conjugated at a 1:1 molar ratio with mSA, for 5 min at 24 ºC. Neurons were washed 4x with Tyrode's and then imaged live. Colocalization of QDs with synapses[14, 29] was calculated by first masking the QD pixels with a signal above background (to give the "QD mask"). Next, the Homer-GFP pixels were masked to include synaptic puncta but to exclude most of the diffuse low-intensity GFP signal in the dendritic shafts (to give the "GFP mask"). An intersection mask was created by crossing the QD and GFP masks, to isolate the QD pixels that overlapped with GFP-positive synaptic puncta. The corrected total QD intensities under each mask were obtained after background subtraction. Colocalization percentages were calculated by dividing the QD total intensity under the "intersection mask" by the QD total intensity under the "QD mask". The Alexa Fluor 568 signal was masked and analyzed in the same way as for QDs. The analysis was performed for 6 separate images, for each labeling condition (18 images in total). Not all GluR2 is expected to be synaptically localized and the colocalization observed for mSA-Alexa Fluor 568 was comparable to the value previously obtained using immunofluorescence staining (69 ± 11%)[30]. Significance was determined using Student's t-test (two-tailed).

Single molecule imaging of LDL receptor (Supplementary Videos 1 and 2, and Supplementary Figure 6)

COS7 cells were transfected with 0.1 μg *wild-type* or *mutant AP-LDL receptor*, 0.1 μg *BirA-ER* and 5 ng *BFP* per well of a 48-well plate and incubated with 10 μM biotin. The

next day, cells were washed 3x in PBS and incubated with 10 nM sQD-mSA$_1$ for 5 min at 24 ºC. Cells were washed 4x in PBS and imaged immediately at 37 °C.

Reference List

1. Dabbousi,B.O. *et al.* (CdSe)ZnS core-shell quantum dots: Synthesis and characterization of a size series of highly luminescent nanocrystallites. *Journal of Physical Chemistry B* **101**, 9463-9475 (1997).
2. Fisher,B.R., Eisler,H.J., Stott,N.E., & Bawendi,M.G. Emission intensity dependence and single-exponential behavior in single colloidal quantum dot fluorescence lifetimes. *Journal of Physical Chemistry B* **108**, 143-148 (2004).
3. Uyeda,H.T., Medintz,I.L., Jaiswal,J.K., Simon,S.M., & Mattoussi,H. Synthesis of compact multidentate ligands to prepare stable hydrophilic quantum dot fluorophores. *Journal of the American Chemical Society* **127**, 3870-3878 (2005).
4. Graff,C.P., Chester,K., Begent,R., & Wittrup,K.D. Directed evolution of an anti-carcinoembryonic antigen scFv with a 4-day monovalent dissociation half-time at 37 degrees C. *Protein Eng Des Sel* **17**, 293-304 (2004).
5. Howarth,M. *et al.* A monovalent streptavidin with a single femtomolar biotin binding site. *Nat. Methods* **3**, 267-273 (2006).
6. Howarth,M. & Ting,A.Y. Imaging proteins in live mammalian cells with biotin ligase and monovalent streptavidin. *Nat. Protoc.* **3**, 534-545 (2008).
7. Sapsford,K.E. *et al.* Kinetics of metal-affinity driven self-assembly between proteins or peptides and CdSe-ZnS quantum dots. *Journal of Physical Chemistry C* **111**, 11528-11538 (2007).
8. Magde,D., Elson,E.L., & Webb,W.W. Fluorescence correlation spectroscopy. II. An experimental realization. *Biopolymers* **13**, 29-61 (1974).
9. Larson,D.R. *et al.* Water-soluble quantum dots for multiphoton fluorescence imaging in vivo. *Science* **300**, 1434-1436 (2003).
10. Schwille,P., Oehlenschlager,F., & Walter,N.G. Quantitative hybridization kinetics of DNA probes to RNA in solution followed by diffusional fluorescence correlation analysis. *Biochemistry* **35**, 10182-10193 (1996).
11. Eaton,D.F. Reference Materials for Fluorescence Measurement. *Pure and Applied Chemistry* **60**, 1107-1114 (1988).
12. Goldman,E.R. *et al.* Self-assembled luminescent CdSe-ZnS quantum dot bioconjugates prepared using engineered poly-histidine terminated proteins. *Analytica Chimica Acta* **534**, 63-67 (2005).
13. Liu,W. *et al.* Compact biocompatible quantum dots functionalized for cellular imaging. *J. Am. Chem. Soc.* **130**, 1274-1284 (2008).
14. Howarth,M., Takao,K., Hayashi,Y., & Ting,A.Y. Targeting quantum dots to surface proteins in living cells with biotin ligase. *Proc. Natl. Acad. Sci. U. S. A* **102**, 7583-7588 (2005).
15. Platani,M., Goldberg,I., Lamond,A.I., & Swedlow,J.R. Cajal body dynamics and association with chromatin are ATP-dependent. *Nat. Cell Biol.* **4**, 502-508 (2002).

16. Chen,I., Howarth,M., Lin,W., & Ting,A.Y. Site-specific labeling of cell surface proteins with biophysical probes using biotin ligase. *Nat. Methods* **2**, 99-104 (2005).
17. Munro,S. & Pelham,H.R. A C-terminal signal prevents secretion of luminal ER proteins. *Cell* **48**, 899-907 (1987).
18. Parrott,M.B. & Barry,M.A. Metabolic biotinylation of secreted and cell surface proteins from mammalian cells. *Biochem. Biophys. Res. Commun.* **281**, 993-1000 (2001).
19. Nesbeth,D. *et al.* Metabolic biotinylation of lentiviral pseudotypes for scalable paramagnetic microparticle-dependent manipulation. *Mol. Ther.* **13**, 814-822 (2006).
20. Barat,B. & Wu,A.M. Metabolic biotinylation of recombinant antibody by biotin ligase retained in the endoplasmic reticulum. *Biomol. Eng* **24**, 283-291 (2007).
21. Gama,L. & Breitwieser,G.E. Generation of epitope-tagged proteins by inverse polymerase chain reaction mutagenesis. *Methods Mol. Biol.* **182**, 77-83 (2002).
22. Lehrman,M.A., Goldstein,J.L., Brown,M.S., Russell,D.W., & Schneider,W.J. Internalization-defective LDL receptors produced by genes with nonsense and frameshift mutations that truncate the cytoplasmic domain. *Cell* **41**, 735-743 (1985).
23. Hobbs,H.H., Russell,D.W., Brown,M.S., & Goldstein,J.L. The LDL receptor locus in familial hypercholesterolemia: mutational analysis of a membrane protein. *Annu. Rev. Genet.* **24**, 133-170 (1990).
24. Krieger,M., Brown,M.S., & Goldstein,J.L. Isolation of Chinese hamster cell mutants defective in the receptor-mediated endocytosis of low density lipoprotein. *J. Mol. Biol.* **150**, 167-184 (1981).
25. Baumgartner,M.R. *et al.* Isolated 3-methylcrotonyl-CoA carboxylase deficiency: evidence for an allele-specific dominant negative effect and responsiveness to biotin therapy. *Am. J. Hum. Genet.* **75**, 790-800 (2004).
26. Loike,J.D. & Silverstein,S.C. A fluorescence quenching technique using trypan blue to differentiate between attached and ingested glutaraldehyde-fixed red blood cells in phagocytosing murine macrophages. *J. Immunol. Methods* **57**, 373-379 (1983).
27. Sahlin,S., Hed,J., & Rundquist,I. Differentiation between attached and ingested immune complexes by a fluorescence quenching cytofluorometric assay. *J. Immunol. Methods* **60**, 115-124 (1983).
28. Grecco,H.E. *et al.* Ensemble and single particle photophysical properties (two-photon excitation, anisotropy, FRET, lifetime, spectral conversion) of commercial quantum dots in solution and in live cells. *Microsc. Res. Tech.* **65**, 169-179 (2004).
29. Groc,L. *et al.* Differential activity-dependent regulation of the lateral mobilities of AMPA and NMDA receptors. *Nat. Neurosci.* **7**, 695-696 (2004).
30. Passafaro,M., Piech,V., & Sheng,M. Subunit-specific temporal and spatial patterns of AMPA receptor exocytosis in hippocampal neurons. *Nat. Neurosci.* **4**, 917-926 (2001).